Science of Sintering, **54** (2022) 425-438

https://doi.org/10.2298/SOS2204425R

UDK: 666.3.019; 622.785

Artificial Neural Network Applied on Sintered $BaTiO_3$-Ceramic Density

Branislav M. Ranđelović[1,2*)], Srđan Ribar[3], Vojislav V. Mitić[1], Bojana Marković[1], Hans Fecht[4], Branislav Vlahović[5]
[1]University of Nis, Faculty of Electronic Engineering, Nis, Serbia,
[2]University of K. Mitrovica, Faculty of Teachers Education, Leposavić, Serbia
[3]University of Belgrade, Faculty of Mechanical Engineering, Belgrade, Serbia
[4]Instititute of Functional Nanosystems, University of Ulm, Ulm, Germany
[5]North Carolina Central University (NCCU), Durham, N. Carolina, USA

Abstract:
It is very important to determine microstructure parameters of consolidated ceramic samples, because it opens new frontiers for further microelectronics miniaturization and integrations. Therefore, controlling, predicting and designing the ceramic materials' properties are the objectives in ceramic materials consolidating process, within the science of sintering. In order to calculate the precise values of desired microstructure parameter at the level of the grains' coating layers based on the measurements on the bulk samples, we applied the artificial neural networks, as a powerful mathematical tool for mapping input-output data. Input signals are propagated forward, as well as the adjustable coefficients that contribute the calculated output signal, denoted as error, which is propagated backwards and replaced by examined parameter. In our previous research, we used neural networks to calculate different electrophysical parameters at the nano level of the grain boundary, like relative capacitance, breakdown voltage or tangent loss, and now we extend the research on sintered material's density calculation. Errors on the network output were substituted by different consolidated samples density values measured on the bulk, thus enabling the calculation of precise material's density values between the layers. We performed the neural network theoretical experiments for different number of neurons in hidden layers, according to experimental ceramics material's density of $\rho=5.4x10^3 [kg/m^3]$*, but it opens the possibility for neural networks application within other density values, as well.*
Keywords*: Neural network; Ceramics materials; Sintering; Density; Error.*

1. Introduction

Back propagation neural network (BP) is a type of neural network where the output signal - error is propagated backwards, from output to input, spreading throughout the whole network, which allows the calculation of error as the contribution of all network elements [1-4]. The desired input – output mapping is obtained by the neural network training process, resulting in error decrease. Adjustable coefficients, called weights, influence the error value, so this training procedure is applied to adjust these parameters. At the beginning, weights are set to random values, thus the output error is significant, and then by adjusting the coefficients

*) **Corresponding author:** bane@elfak.ni.ac.rs

towards reducing the error, which implies numerous repeating, all input-output data are mapped within the domain of predefined error.
Artificial neural network (ANN) is comprised of neurons that receive input signals, forming input layer, and neurons that generate output signal, forming output layer. Between these two layers, there are different numbers of neurons organized in one or more hidden layers (Fig. 1).

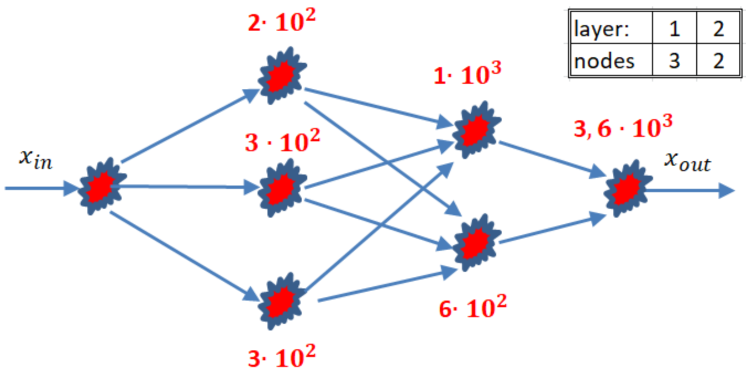

Fig. 1. An example of a neural network.

The micro ceramic material can be observed as a structure constitutes of multiple thin layer coatings around the grains that are mutually interconnected. If we observe the sintered material's structure as a neural network, with grains of the ceramic material represented by network neurons, we can calculate any parameter at the submicron level in thin layers between the grains, based on the experimentally obtained relating characteristics at the bulk sample's surface. ANN method is applied by splitting the bulk sample into equally distant layers, whereby the more layers present; the more precise results are obtained. The error that occurs on the network output, which is the difference between desired and actual output, is replaced by the measured parameter and spread backwards.

In accordance with our previous research, where we applied this method for calculating various ceramics microelectronic characteristics [5-8], we now proceed with the density calculation [9-12] within consolidated $BaTiO_3$-ceramic samples for different consolidation parameters, like sintering temperature, because the consolidation process thermal conditions are very important for material's density.

The network error is a general, nominally useful signal, because any ceramic material's parameter (including density) could be defined as an output error. The lower calculated errors mean that we get more precise values of the examined parameter at the grain boundaries level. Also, it is very important to calculate the error distribution regarding all hidden layer nodes. Therefore, summarizing of all network nodes errors and calculating number of nodes related distribution has to be done, in order to obtain deviations regarding the starting error. Summarizing of error values regarding layers and calculating number of nodes related distribution for layers, has to be performed, as well.

2. Materials and Experimental Procedures

In this experiment, we applied process to high purity $BaTiO_3$ Murata powder [13], with mean grain size < 2 μm, and 99.9 % purity. Four steps in ceramic powder preparation process (for sintering consolidation of $BaTiO_3$ - ceramics samples) were done: measuring and forming starting powders mixture; wet mixing and spraying; molding and process control; and preparation, samples sintering and process control. Duration of homogenization of organic binders in powder mixture was about 48 h. The mass, processed into a mill with a balls and water, was transferred by a membrane pump and dried. So, we obtained a desired powder granulation. We tested the material density every hour, using a special vessel and we applied vibrating sieve afterwards. Diameters of powder particles were 10-130 μm.

We analyzed various sintering temperatures (1190-1370^{o}C), length of time (2-3 h) and impact of different additives (CeO_2, $MnCO_3$). But in this analysis, we were focused on relation with pressures of 86 MPa and density.

We created several different neural networks with two hidden layers, and since the dimensions of the ceramic samples are $h = (0{,}57 \pm 0{,}05) \cdot 10^{-3} m, d = 16{,}5 \cdot 10^{-3} m$, we can calculate the distance between layers. In this research, the output error was replaced by density values experimentally obtained during the sintering process, and due to spreading it through the whole network, calculation of intergranular density was successfully performed.

Tab. I Extract of experimental results.

sample type	*P [MPa]*	*ρ [kg/m³]*
$BaTiO_3$ – ceramics with basic mixture	86	$5.4x10^3$
$BaTiO_3$ -ceramics: composition 0.1%CeO_2+0.14%$MnCO_3$	86	$3.2x10^3$
$BaTiO_3$ -ceramics: composition 0.1%CeO_2	86	$3.4x10^3$

In further analysis and theoretical experiment, we will use just the data from the first raw of the Tab. I. ρ=$5.4x10^3 [kg/m^3]$.

3. Results and Discussion

Twelve different two-layer neural networks were developed, with *n=6,8,10* neurons in the first hidden layer and *m=2,4,6,8,10* neurons in the second hidden layer. Density in hidden layers (ρ), as well as errors calculated during the training process for each example, will be discussed.

For a neural network with 6 neurons in the 1st hidden layer and 2 neurons in the 2nd hidden layer (Fig. 2.), density ρ and errors calculated in the training process are presented in Tab. II.

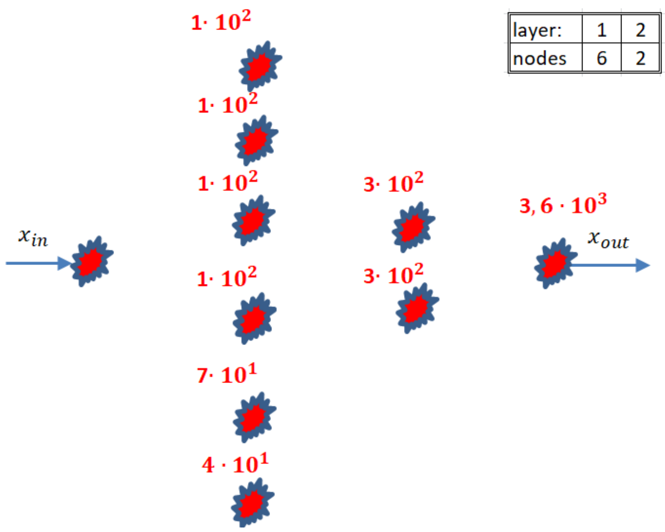

Fig. 2. Neural network with 6 neurons in the 1st hidden layer and 2 neurons in the 2nd hidden layer.

Tab. II Density **ρ** and calculated errors for a neural network with 6 neurons in the 1st hidden layer and 2 neurons in the 2nd hidden layer.

	Density ρ			**Calculated error**		
neuron	1st hidden layer	2nd hidden layer	output neuron	1st hidden layer	2nd hidden layer	output neuron
1	167	534	5400	-0.01403	-0.04491	0.453992
2	183	488		-0.01539	-0.04103	
3	212			-0.01786		
4	157			-0.01319		
5	111			-0.0093		
6	66			-0.00553		

For a neural network with 6 neurons in the 1st hidden layer and 4 neurons in the 2nd hidden layer (Fig. 3.), density ρ and errors calculated in the training process are presented in Tab. III.

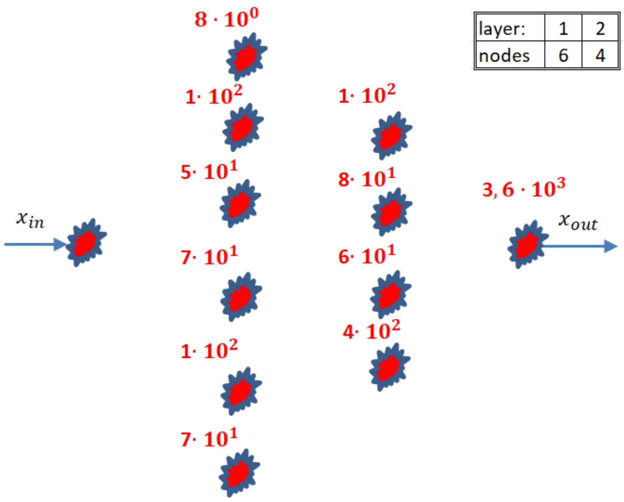

Fig. 3. Neural network with 6 neurons in the 1st hidden layer and 4 neurons in the 2nd hidden layer.

Tab. III Density **ρ** and calculated errors for a neural network with 6 neurons in the 1st hidden layer and 4 neurons in the 2nd hidden layer.

	density ρ			calculated error		
neuron	1st hidden layer	2nd hidden layer	output neuron	1st hidden layer	2nd hidden layer	output neuron
1	12	233	5400	0.001788	0.03584	0.82996
2	144	124		0.022182	0.01907	
3	80	90		0.012296	0.013913	
4	100	546		0.015452	0.083917	
5	167			0.02568		
6	107			0.016528		

For a neural network with 6 neurons in each of two hidden layers (Fig. 4.), density ρ and errors calculated in the training process are presented in Tab. IV.

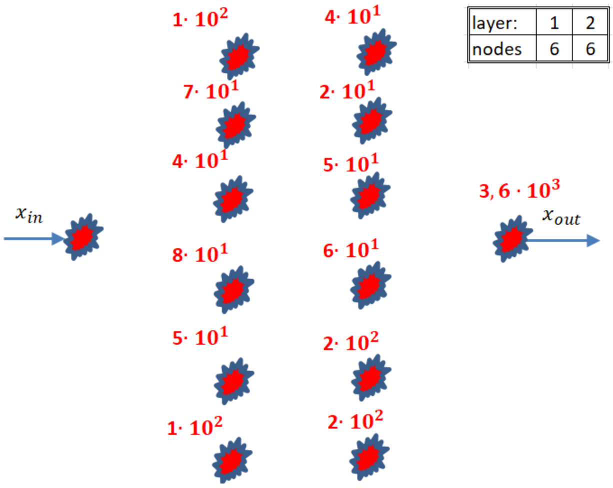

Fig. 4. Neural network with 6 neurons in each hidden layer.

Tab. IV Density ρ and calculated errors for a neural network with 6 neurons in each hidden layer.

neuron	density ρ			calculated error		
	1st hidden layer	2nd hidden layer	output neuron	1st hidden layer	2nd hidden layer	output neuron
1	146	62	5400	0.023166	0.00987	0.854657
2	99	31		0.015662	0.004984	
3	54	77		0.008554	0.012138	
4	119	86		0.018826	0.013589	
5	77	345		0.012209	0.054632	
6	147	258		0.023209	0.040835	

For a neural network with 8 neurons in the 1st hidden layer and 2 neurons in the 2nd hidden layer (Fig. 5.), density ρ and errors calculated in the training process are presented in Tab. V.

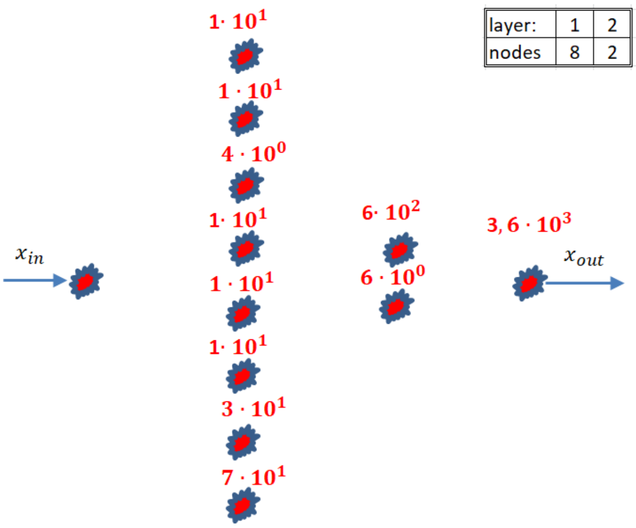

Fig. 5. Neural network with 8 neurons in the 1st hidden layer and 2 neurons in the 2nd hidden layer.

Tab. V Density **ρ** and calculated errors for a neural network with 8 neurons in the 1st hidden layer and 2 neurons in the 2nd hidden layer.

neuron	density ρ			calculated error		
	1st hidden layer	2nd hidden layer	output neuron	1st hidden layer	2nd hidden layer	output neuron
1	13	86	5400	0.002562	0.016469	1.033113
2	17	-8.6		0.003207	-0.00165	
3	5			0.00105		
4	16			0.002997		
5	17			0.00329		
6	20			0.003841		
7	5			10.000948		
8	10			0.001996		

For a neural network with 8 neurons in the 1st hidden layer and 4 neurons in the 2nd hidden layer (Fig. 6.), density ρ and errors calculated in the training process are presented in Tab. VI.

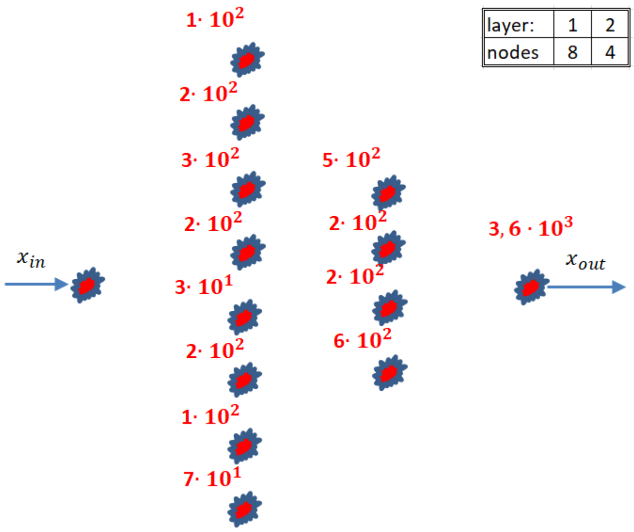

Fig. 6. Neural network with 8 neurons in the 1st hidden layer and 4 neurons in the 2nd hidden layer.

Tab. VI Density **ρ** and calculated errors for a neural network with 8 neurons in the 1st hidden layer and 4 neurons in the 2nd hidden layer.

neuron	density ρ			calculated error		
	1st hidden layer	2nd hidden layer	output neuron	1st hidden layer	2nd hidden layer	output neuron
1	183	763	5400	-0.00941	-0.03926	0.277903
2	248	259		-0.01278	-0.01333	
3	397	267		-0.02044	-0.01376	
4	280	915		-0.01442	-0.04708	
5	50			-0.0026		
6	299			-0.01538		
7	217			-0.01117		
8	101			-0.00522		

For a neural network with 8 neurons in the 1st hidden layer and 6 neurons in the 2nd hidden layer (Fig. 7.), density ρ and errors calculated in the training process are presented in Tab.VII.

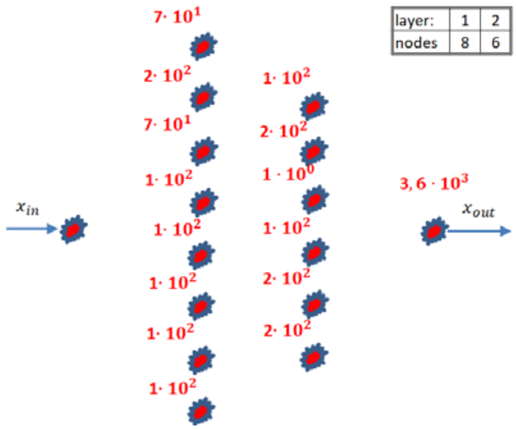

Fig. 7. Neural network with 8 neurons in the 1st hidden layer and 6 neurons in the 2nd hidden layer.

Tab. VII Density **ρ** and calculated errors for a neural network with 8 neurons in the 1st hidden layer and 6 neurons in the 2nd hidden layer.

	density ρ			calculated error		
neuron	1st hidden layer	2nd hidden layer	output neuron	1st hidden layer	2nd hidden layer	output neuron
1	100	160	5400	0.004279	0.00685	0.231791
2	245	289		0.010532	0.012422	
3	106	201		0.00456	0.008261	
4	197	227		0.008476	0.009762	
5	203	278		0.008735	0.011928	
6	138	264		0.005924	0.011353	
7	210			0.009023		
8	225			0.009646		

For a neural network with 8 neurons per each hidden layer (Fig. 8.), density ρ and errors calculated in the training process are presented in Tab. VIII.

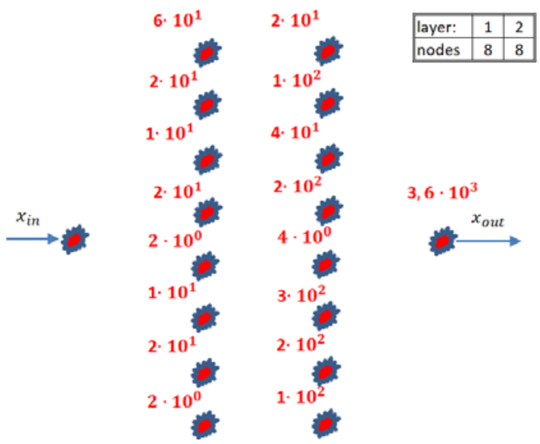

Fig. 8. Neural network with 8 neurons pear each hidden layer.

Tab. VIII Density ρ and calculated errors for a neural network with 8 neurons per each hidden layer.

neuron	density ρ			calculated error		
	1st hidden layer	2nd hidden layer	output neuron	1st hidden layer	2nd hidden layer	output neuron
1	89	-36	5400	0.018174	-0.00718	1.103968
2	38	198		0.007725	0.040433	
3	-23	-60		-0.00461	-0.01225	
4	-27	-250		-0.00561	-0.05107	
5	2.4	6.7		0.000492	0.001369	
6	18	391		0.003766	0.079895	
7	-24	-297		-0.00493	-0.06065	
8	2.8	163		0.000567	0.033305	

For a neural network with 10 neurons in the 1st hidden layer and 2 neurons in the 2nd hidden layer (Fig. 9.), density ρ and errors calculated in the training process are presented in Tab. IX.

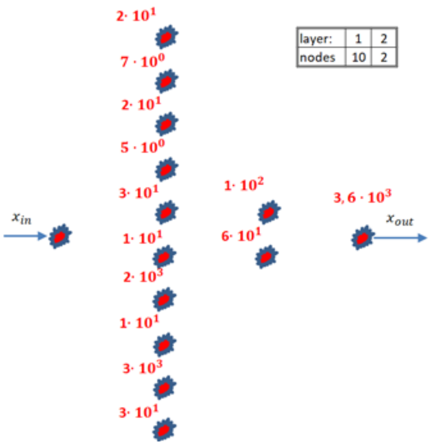

Fig. 9. Neural network with 10 neurons in the 1st hidden layer and 2 neurons in the 2nd hidden layer.

Tab. IX Density **ρ** and calculated errors for a neural network with 10 neurons in the 1st hidden layer and 2 neurons in the 2nd hidden layer.

neuron	density ρ			calculated error		
	1st hidden layer	2nd hidden layer	output neuron	1st hidden layer	2nd hidden layer	output neuron
1	26	191	5400	0.00461	0.033537	0.941893
2	10	86		0.001767	0.015042	
3	31			0.005505		
4	7			0.001252		
5	50			0.00885		
6	19			0.003371		
7	27			0.004735		
8	20			0.003593		
9	40			0.007073		
10	48			0.008367		

For a neural network with 10 neurons in the 1st hidden layer and 4 neurons in the 2nd hidden layer (Fig. 10.), density ρ and errors calculated in the training process are presented in Tab. X.

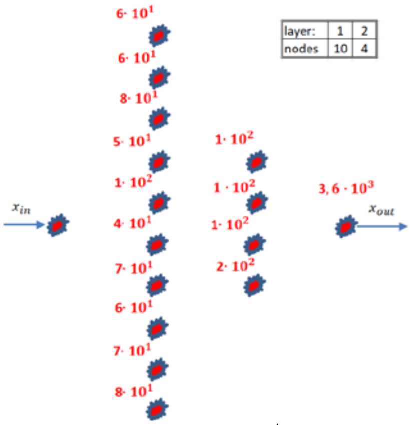

Fig. 10. Neural network with 10 neurons in the 1st hidden layer and 4 neurons in the 2nd hidden layer.

Tab. X Density **ρ** and calculated errors for a neural network with 10 neurons in the 1st hidden layer and 4 neurons in the 2nd hidden layer.

	density ρ			calculated error		
neuron	1st hidden layer	2nd hidden layer	output neuron	1st hidden layer	2nd hidden layer	output neuron
1	96	231	5400	-0.00834	-0.02009	0.469675
2	93	151		-0.00807	-0.01315	
3	112	187		-0.00991	-0.01627	
4	70	259		-0.006	-0.02257	
5	140			-0.01216		
6	62			-0.00537		
7	99			-0.0086		
8	95			-0.0083		
9	103			-0.00892		
10	116			-0.01007		

For a neural network with 10 neurons in the 1st hidden layer and 6 neurons in the 2nd hidden layer (Fig. 11.), density ρ and errors calculated in the training process are presented in Tab. XI.

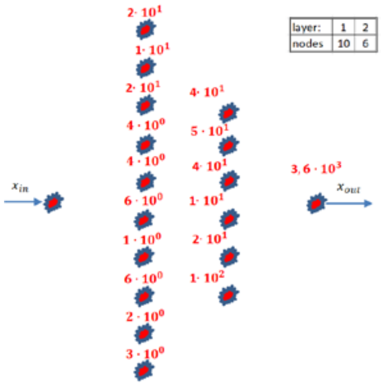

Fig. 11. Neural network with 10 neurons in the 1st hidden layer and 6 neurons in the 2nd hidden layer.

Tab. XI Density **ρ** and calculated errors for a neural network with 10 neurons in the 1st hidden layer and 6 neurons in the 2nd hidden layer.

neuron	1st hidden layer	2nd hidden layer	output neuron	1st hidden layer	2nd hidden layer	output neuron
1	25	54	5400	-0.00502	0.011114	1.102478
2	13	82		-0.00274	0.016747	
3	30	60		0.0062	0.01213	
4	6	22		0.001284	-0.00441	
5	6	36		-0.00128	-0.00732	
6	9	178		-0.00179	-0.03631	
7	1			-0.00027		
8	9			0.001758		
9	3			-0.00072		
10	5			0.000972		

For a neural network with 10 neurons in the 1st hidden layer and 8 neurons in the 2nd hidden layer (Fig. 12.), density ρ and errors calculated in the training process are presented in Tab. XII.

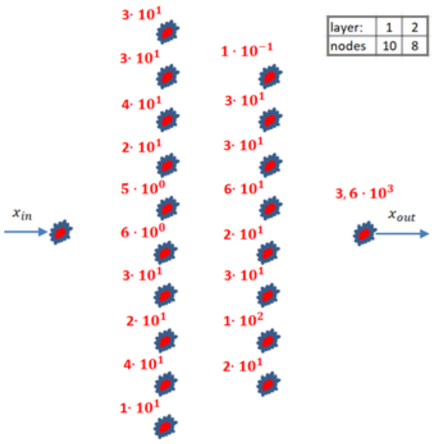

Fig. 12. Neural network with 10 neurons in the 1st hidden layer and 8 neurons in the 2nd hidden layer.

Tab. XII Density **ρ** and calculated errors for a neural network with 10 neurons in the 1st hidden layer and 8 neurons in the 2nd hidden layer.

	density ρ			calculated error		
neuron	1st hidden layer	2nd hidden layer	output neuron	1st hidden layer	2nd hidden layer	output neuron
1	44	0.1	5400	0.006593	0.000244	0.814185
2	47	44		0.007172	0.006576	
3	65	-44		30.009782	-0.00668	
4	37	95		0.005601	0.014368	
5	7	-35		0.001046	-0.00531	
6	9	40		0.001348	0.005974	
7	48	175		0.007255	0.026401	
8	31	26		0.004759	0.00394	
9	64			0.00968		
10	23			0.003473		

For a neural network with 10 neurons per each of two hidden layers (Fig. 13.), density *ρ* and errors calculated in the training process are presented in Tab. XIII.

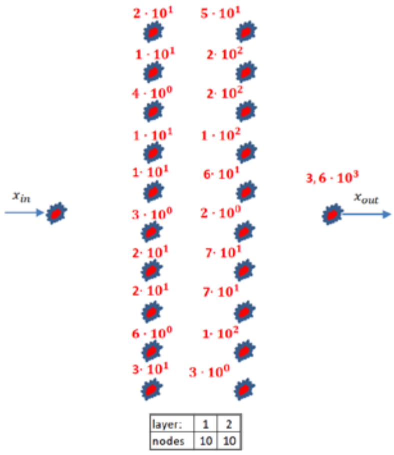

Fig. 13. Neural network with 10 neurons per each hidden layer.

Tab. XIII Density ρ and calculated errors for a neural network with 10 neurons per each hidden layer.

	density ρ			calculated error		
neuron	1^{st} hidden layer	2^{nd} hidden layer	output neuron	1^{st} hidden layer	2^{nd} hidden layer	output neuron
1	30	83	5400	0.005439	0.014923	0.9711
2	16	281		-0.0029	0.050599	
3	6	264		0.001052	-0.04746	
4	17	151		0.003093	0.027248	
5	21	94		0.003788	0.017005	
6	4	3		-0.00082	-0.0005	
7	25	105		0.004431	0.018842	
8	27	113		0.004794	-0.02038	
9	9	184		-0.00161	-0.03316	
10	48	4		0.008662	-0.0008	

Based on the theoretical experiment results presented in Fig. 2-13, we demonstrated successful application of the neural network method on samples' surface density calculation, as an original novelty with many advantages in this field [14-22].

4. Conclusion

Determining microstructure parameters of consolidated ceramic samples is very important, because it opens new frontiers for further microelectronics miniaturization and integrations. In this paper, back propagation neural network is applied, to calculate density values in the coating layers between the micro ceramics material's grains. Calculation is based on experimental density measurements on the bulk sample for $\boldsymbol{\rho}=5.4x10^3 [kg/m^3]$. This is new and innovative approach in calculation and determination of characteristics of the materials, at the intergranular nano level. In order to calculate the precise values of desired parameter, based on the measurements on the bulk samples, we applied the artificial neural networks, as a powerful mathematical tool for mapping input-output data. Unlike mathematical a method which provides statistical parameters' values within the whole sintered sample, BP method enables the calculation of precise density values at the material's grains and pores boundary level. In this paper is assumed that neural network nodes present ceramic grains. In that case increase of neural network complexity should provide better density estimation. One can notice that better uniformity of grains density is achieved as neural network complexity rises.

This opens new perspectives in further miniaturization of micro ceramics materials and also provides advanced technology development, within the science of sintering. The application of BP neural network also opens new possibilities for very precisely predicting and designing the ceramic materials properties and desired microstructure density [23], at the nano level. Those results are natural continuation of the results from previous papers in this area. They are also a new path to a variety of interesting possibilities for further research.

5. References

1. Rumelhart, D., *et al.* Learning representations by back-propagation errors, *Nature*, 323, (1986) 533-536
2. da Silva I.N., et al. Artificial Neural Network Architectures and Training Processes, in: *Artificial Neural Networks*. Springer, Cham., (2017) 21-28
3. Ribar S. *et al*. Neural Networks Application on Human Skin Biophysical Impedance Characterizations, *Biophysical Reviews & Letters*, 16 (2021) 2021-19
4. Hecht-Nielsen: Theory of the backpropagation neural network, International Joint Conference on Neural Networks, IJCNN, Washington, D. C., USA, 1989. Vol. 1, pp 593-605
5. Mitic V. V., *et al*. The Artificial Neural Networks Applied for Microelectronics Intergranular Relations Determination, *Integrated Ferroelectics*, 212 (2020) 135-146.
6. Mitic V. V., *et al*. Neural Networks and Microelectronics Parameters Distribution Measurements Depending on Sintering Temperature and Applied Voltage, MPL B, 34 (35) (2020) 2150172.
7. Vidak Vasic M., *et al*. An Artificial Neural Network-based Prediction Model for Utilization of Coal Ash in Production of Fired Clay Bricks: A review, Science of Sintering, 53 (1) (2021) 37-53.
8. Randjelovic B., *et al*. "Ceramics, Materials, Microelectronics and Graph Theory new Frontiers", MPLB, Vol 34 (34) (2020) 2150159.
9. Mitic V. V., *et al*. Entropy and fractal nature, *Thermal Science*, 24 3B (2020) 2203-2212.
10. Mitic V. V., *et al***., "**Butler-Volmer Current Equation and Fractal Nature Correction in Electrochemical Energy", *Thermal Science*, **(**2020) 232-232,
11. Randjelovic B., *et al*. "Graph Theory Approach in Synthetized Diamonds Electrophysical Parameters Defining", in: *Bioceramics, Biomimetic and other Compatible Materials Features for Medical Applications*, (Ed. Najman S., Mitic V., Groth T., Barbeck M., Yu Chen P., Sun Z.), Springer Nature, Cham, Switzerland, 2021, accepted for publication
12. Ribar S., *et al*. "Neural Networks from Biophysical Applications in Microelectronics Parameters Measurements", in: *Bioceramics, Biomimetic and other Compatible Materials Features for Medical Applications,* (Ed. Najman S., Mitic V., Groth T., Barbeck M., Yu Chen P., Sun Z.), Springer Nature, Cham, Switzerland, 2021, accepted for publication

13. Mitic V.V., Structure and electrical properties of $BaTiO_3$ ceramics, (in Serbian), Zaduzbina Andrejevic, Belgrade, Serbia, 2001, pp. 35.
14. Mitić V. V *et al.* "The 3D graph approach for breakdown voltage calculation in $BaTiO_3$ ceramics", IJMPB, Vol 35 (7) (2021) 2150103.
15. Mitić V. V *et al.* "Graph Theory Applied to Microelectronic Intergranular Relations", Ferroelectrics, 570 (2021) 145-152.
16. Mitić V. V *et al.*, "Fractal Microeletronic Frontiers and Graph Theory Applications", Int.Conference MS&T 2019, Book of Abstracts, Portland, USA, 29 September – 03 October 2019.
17. Mitić V. V *et al.*,"Investigation of intergranular dielectric properties within the relation between fractal, graph and neural networks theories", Int.Conf. Electronic Materials and Applications EMA-2021, Virtual, January 19-21, 2021.
18. Mitić V. V *et al.* "Fractal, graph and neural network theories applied on $BaTiO_3$ electronic ceramics", Int.Conf. Electronic Materials and Applications EMA-2021, Virtual, January 19-21, 2021.
19. Mitić V. V *et al.*, "Neural networks and applied graph theory approaches for intergranular properties measurements investigation", Int.Conf. Electronic Materials and Applications EMA-2021, Virtual, January 19-21, 2021.
20. Mitić V. V *et al.* "3D graph theory application on modified nano $BaTiO_3$ electronic ceramics", Int.Conf. Electronic Materials and Applications EMA-2021, Virtual, January 19-21, 2021.
21. Mitic V. V *et al.* "Sinterign Temperature Influenceo on Grains Function Distribution by Neural Network Application", Thermal Science (2021) (accepted).
22. Filipovic S., *et al*, Multiferroic Heterostrucutre $BaTiO_3$/ε-Fe_2O_3 Composite Obtained by in situ Reaction, Science of Sintering, 53 (1) (2021) 1-8.
23. Ribar S. *et al.* "*The Neural Network Application on Ceramics Materials Density*", Int.Conf. IcETRAN 2021, September 08-10, 2021.

Сажетак: *Одређивање параметара микроструктуре консолидованих керамичких узорака је веома важно, јер то отвара нове могућности за даљу минијатуризацију и интеграције. Према томе, контрола, предвиђање и пројектовање својстава керамичких материјала су циљеви у процесу консолидације керамичких материјала, у оквиру науке о синтеровању. Да бисмо израчунали прецизне вредности жељеног микроструктурног параметра на нивоу слојева зрна, на основу мерења на масовним узорцима, применили смо вештачке неуронске мреже, као моћан математички алат за мапирање улазно-излазних података. Улазни сигнали се пропагирају напред, као и подесиви коефицијенти који доприносе израчунатом излазном сигналу, означеном као грешка, који се шири уназад и замењује испитиваним параметром. У нашем претходном истраживању користили смо неуронске мреже за израчунавање различитих електрофизичких параметара на нано нивоу границе зрна, као што су релативни капацитет, напон пробоја или тангентни губитак, а сада проширујемо истраживање на прорачун густине синтерованог материјала. Грешке на излазу мреже су замењене различитим вредностима густине консолидованих узорака измереним на маси, чиме је омогућено израчунавање прецизних вредности густине материјала између слојева. Изводили смо теоријске експерименте са неуронским мрежама за различит број неурона у скривеним слојевима, према густини експерименталног керамичког материјала од* $\rho=5,4x10^3[kg/m^3]$*, али то отвара могућност примене неуронских мрежа и у оквиру других вредности густине.*

Кључне речи*:* *неуронска мрежа, керамички материјали, синтеровање, густина, грешка.*